Bollettino
Unione Matematica Italiana

Simone Scacchi

Scalable Block Preconditioners for the Parabolic-Elliptic Bidomain coupling

Bollettino dell'Unione Matematica Italiana, Serie 9, Vol. **6** (2013), n.3, p. 699–714.

Unione Matematica Italiana

<http://www.bdim.eu/item?id=BUMI_2013_9_6_3_699_0>

Bollettino dell'Unione Matematica Italiana, Unione Matematica Italiana, 2013.

Bollettino U. M. I.
(9) **VI** (2013), 699-714

Scalable Block Preconditioners for the Parabolic-Elliptic Bidomain coupling

S. SCACCHI

Abstract. – *We review some results on parallel multilevel block preconditioners for the Bidomain model of electrocardiology. This model describes the bioelectric activity of the cardiac tissue in terms of the transmembrane electric potential v and the extracellular electric potential u_e and it consists of a system of a parabolic non-linear partial differential equation (PDE) for v and an elliptic linear PDE for u_e. The two PDEs are coupled with a system of ordinary differential equations, modeling the cellular membrane ionic currents. The space and time discretization of the Bidomain system yields at each time step the solution of large and ill-conditioned linear systems. We analyze here the scalability of Multilevel Schwarz Block-Diagonal and Block-Factorized preconditioners for the discrete Bidomain system. New three-dimensional parallel numerical tests on a Linux cluster are performed to compare the Multilevel Schwarz block preconditioners with Block Jacobi (BJ) and Algebraic Multigrid (AMG) preconditioners. The results show that the preconditioners developed are scalable and more efficient than both BJ and AMG preconditioners.*

1. – Introduction

We construct and analyze multilevel block preconditioners for implicit-explicit (IMEX) time discretizations of the Bidomain model of electrocardiology. The Bidomain model describes the cardiac bioelectric activity and consists of a parabolic non-linear reaction-diffusion PDE, coupled with an elliptic linear PDE. The unknowns are the transmembrane electric potential v and the extracellular potential u_e. The two PDEs are coupled through the non-linear reaction term with a stiff system of ordinary differential equations (ODEs), the so-called membrane model, describing the ionic currents through the cellular membrane.

The different space and time scales involved make the solution of this problem very challenging. Several approaches have been developed in order to reduce the high computational costs required by the Bidomain model. Fully implicit methods in time have been considered in a few studies, see e.g. [19, 17, 18, 28] and require the solution of nonlinear systems at each time step. Most previous works have considered IMEX time discretizations and/or operator splitting schemes, where the reaction and diffusion terms are treated separately, see e.g. [5, 6, 9, 15, 25, 32, 37, 38]. The advantage of IMEX

and operator splitting schemes is that they only require the solution of linear systems at each time step. Many different preconditioners have been proposed in order to obtain efficient iterative solvers for such linear systems: block diagonal or triangular [23, 24, 5, 36, 10], optimized Schwarz [11], multigrid [31, 25, 23, 24], multilevel Schwarz [20, 27], Balancing Neumann-Neumann [39] and BDDC [40] preconditioners.

In this work, we review the results obtained in [21] on the scalability of Multilevel Schwarz Block-Diagonal and Block-Factorized preconditioners for the discrete Bidomain system. New three-dimensional parallel numerical tests on a Linux cluster are performed to compare the Multilevel Schwarz block preconditioners with Block Jacobi (BJ) and Algebraic Multigrid (AMG) block preconditioners. The results show that our multilevel preconditioners are scalable and more efficient than both BJ and AMG preconditioners on a whole heart beat simulation.

The rest of the paper is organized as follows: we present the Bidomain model in Section 2 and its time and space discretization in Section 3; in Section 4 and 5, we introduce the Multilevel Schwarz Block-Diagonal and Block-Factorized preconditioners; finally, we report in Section 6 the results of three-dimensional parallel simulations.

2. – The anisotropic Bidomain model

The macroscopic Bidomain representation of the cardiac tissue volume Ω is obtained by considering the superposition of two anisotropic continuous media, the intra- (i) and extra- (e) cellular media, coexisting at every point of the tissue and separated by a distributed continuous cellular membrane; see e.g. [22] for a derivation of the Bidomain model from homogenization of cellular models. We recall that the cardiac tissue consists of an arrangement of fibers that rotate counterclockwise from epi- to endocardium, and that have a laminar organization modeled as a set of muscle sheets running radially from epi- to endocardium. The anisotropy of the intra- and extracellular media, related to the macroscopic arrangement of the cardiac myocytes in the fiber structure, is described by the anisotropic conductivity tensors $D_i(\boldsymbol{x})$ and $D_e(\boldsymbol{x})$, respectively, defined in (2) below.

2.1 – *Continuous model*

We denote by $\Omega \subset \mathbb{R}^3$ the bounded physical region occupied by the cardiac tissue and we introduce the parabolic-elliptic formulation of the Bidomain system. Given an applied extracellular current per unit volume $I^e_{app} : \Omega \times (0,T) \to \mathbb{R}$, and initial conditions $v_0 : \Omega \to \mathbb{R}$, $w_0 : \Omega \to \mathbb{R}^{N_w}$, find the the transmembrane potential $v : \Omega \times (0,T) \to \mathbb{R}$, extracellular potentials $u_e : \Omega \times (0,T) \to \mathbb{R}$, the

gating variables $w : \Omega \times (0,T) \to \mathbb{R}^{N_w}$ and the ionic concentrations $c : \Omega \times (0,T) \to \mathbb{R}^{N_c}$ such that

$$
(1) \qquad \begin{cases}
c_m \dfrac{\partial v}{\partial t} - \operatorname{div}(D_i \nabla v) - \operatorname{div}(D_i \nabla u_e) + I_{ion}(v,w,c) = 0 & \text{in } \Omega \times (0,T) \\
-\operatorname{div}(D_i \nabla v) - \operatorname{div}((D_i + D_e)\nabla u_e) = I^e_{app} & \text{in } \Omega \times (0,T) \\
\dfrac{\partial w}{\partial t} - R(v,w) = 0, & \text{in } \Omega \times (0,T) \\
\dfrac{\partial c}{\partial t} - S(v,w,c) = 0, & \text{in } \Omega \times (0,T) \\
\boldsymbol{n}^T D_i \nabla (v + u_e) = 0 & \text{in } \partial\Omega \times (0,T) \\
\boldsymbol{n}^T (D_i + D_e) \nabla u_e + \boldsymbol{n}^T D_i \nabla v = 0, & \text{in } \partial\Omega \times (0,T) \\
v(\boldsymbol{x},0) = v_0(\boldsymbol{x}), \quad w(\boldsymbol{x},0) = w_0(\boldsymbol{x}), \quad c(\boldsymbol{x},0) = c_0(\boldsymbol{x}) & \text{in } \Omega,
\end{cases}
$$

where c_m is the membrane capacitance per unit volume. The applied extracellular current I^e_{app} must satisfy the compatibility condition $\int_\Omega I^e_{app}\,\mathrm{dx} = 0$, and we impose the reference potential $\int_\Omega u_e\,\mathrm{dx} = 0$. The non-linear reaction term I_{ion} and the ODE system for the gating variables w and the ionic concentrations c are given by the ionic membrane model. Here we will consider the Luo-Rudy I (LR1) membrane model [16]. For the well-posedness analysys of the Bidomain model (1) coupled with complex membrane models as the LR1 model and its recent updates, we refer to [34, 35].

The conductivity tensors $D_i(\boldsymbol{x})$ and $D_e(\boldsymbol{x})$ at any point $\boldsymbol{x} \in \Omega$ are assumed orthotropic, thus defined as

$$
(2) \qquad D_{i,e}(\boldsymbol{x}) \;= \sigma_l^{i,e}\; \boldsymbol{a}_l(\boldsymbol{x})\boldsymbol{a}_l^T(\boldsymbol{x}) + \sigma_t^{i,e}\; \boldsymbol{a}_t(\boldsymbol{x})\boldsymbol{a}_t^T(\boldsymbol{x}) + \sigma_n^{i,e}\; \boldsymbol{a}_n(\boldsymbol{x})\boldsymbol{a}_n^T(\boldsymbol{x}).
$$

Here $\boldsymbol{a}_l(\boldsymbol{x})$, $\boldsymbol{a}_t(\boldsymbol{x})$, $\boldsymbol{a_n}(\boldsymbol{x})$, is a triplet of orthonormal principal axes with $\boldsymbol{a}_l(\boldsymbol{x})$ parallel to the local fiber direction, $\boldsymbol{a}_t(\boldsymbol{x})$ and $\boldsymbol{a}_n(\boldsymbol{x})$ tangent and orthogonal to the radial laminae, respectively, and both being transversal to the fiber axis (see e.g. LeGrice et al. [14]). Moreover, $\sigma_l^{i,e}$, $\sigma_t^{i,e}$, $\sigma_n^{i,e}$ are the conductivity coefficients in the intra- and extracellular media measured along the corresponding directions $\boldsymbol{a}_l$, $\boldsymbol{a}_t$, $\boldsymbol{a}_n$.

2.2 – *Variational formulation*

Let V be the Sobolev space $H^1(\Omega)$, define the spaces

$$
\widetilde{V} = \left\{ \psi \in V : \int_\Omega \psi = 0 \right\} \qquad \text{and} \qquad U = V \times \widetilde{V} = \{ u = (\varphi, \psi) : \varphi \in V, \psi \in \widetilde{V} \},
$$

define the usual L^2-inner product $(\varphi,\psi)=\int_\Omega \varphi\psi dx\ \forall\varphi,\psi\in L^2(\Omega)$, and the elliptic bilinear forms

$$a_{i,e}(\varphi,\psi)=\int_\Omega (\nabla\varphi)^T D_{i,e}(x)\nabla\psi dx,$$

$$a(\varphi,\psi)=\int_\Omega (\nabla\varphi)^T D(x)\nabla\psi dx \quad \forall\varphi,\psi\in H^1(\Omega),$$

where $D=D_i+D_e$ is the bulk conductivity tensor.

The variational formulation of the Bidomain model reads as follows. Given v_0, w_0, $c_0\in L^2(\Omega)$, $I^e_{app}\in L^2(\Omega\times(0,T))$, find $v\in L^2(0,T;V)$, $u_e\in L^2(0,T;\widetilde{V})$, $w\in L^2(0,T;L^2(\Omega)^{N_w})$ and $c\in L^2(0,T;L^2(\Omega)^{N_c})$ such that $\frac{\partial v}{\partial t}\in L^2(0,T;V)$, $\frac{\partial w}{\partial t}\in L^2(0,T;L^2(\Omega)^{N_w})$, $\frac{\partial c}{\partial t}\in L^2(0,T;L^2(\Omega)^{N_c})$ and $\forall t\in(0,T)$

$$(3)\qquad \begin{cases} c_m\dfrac{\partial}{\partial t}(v,\hat v)+a_i(v,\hat v)+a_i(u_e,\hat v)+(I_{ion}(v,w,c),\hat v)=0 \quad \forall\hat v\in V\\ a_i(v,\hat u_e)+a(u_e,\hat u_e)=(I^e_{app},\hat u_e) \quad \forall\hat u_e\in\widetilde{V}\\ \dfrac{\partial}{\partial t}(w,\hat w)-(R(v,w),\hat w)=0, \quad \forall\hat w\in V,\\ \dfrac{\partial}{\partial t}(c,\hat c)-(S(v,w,c),\hat c)=0, \quad \forall\hat c\in V, \end{cases}$$

with the appropriate initial conditions in (1).

3. – Discretization and numerical methods

3.1 – *Space discretization*

System (3) is first discretized in space by the finite element method. Let $\mathcal{T}_h$ be a quasi-uniform triangulation of Ω having maximal diameter h and V_h be an associated conforming finite element space. In this work, we will consider isoparametric trilinear finite elements on hexahedral meshes. Once a finite element basis $\{\varphi_l\}_{l=1}^N$ of V_h is chosen, we denote by $A_{i,e}=\{a^{i,e}_{lj}\}$ the symmetric intra- and extracellular stiffness matrices, and by $M=\{m_{lj}\}$ the mass matrix, with elements

$$a^{i,e}_{lj}=\int_\Omega D_{i,e}\nabla\varphi_j\cdot\nabla\varphi_l\,\mathrm{dx}, \qquad m_{lj}=\int_\Omega \varphi_j\ \varphi_l\,\mathrm{dx}.$$

Applying a standard Galerkin procedure to (3) and using the finite element interpolants of I^e_{app}, I_{ion} associated to the vectors of nodal values $\boldsymbol{I}^e_{app}, \boldsymbol{I}_{ion}$, we obtain the following semi-discrete Bidomain problem, written in compact matrix

form as

$$
(4)\qquad \begin{cases} c_m \mathbb{M} \dfrac{d}{dt}\begin{bmatrix} \boldsymbol{v} \\ \boldsymbol{u}_e \end{bmatrix} + \mathbb{A}\begin{bmatrix} \boldsymbol{v} \\ \boldsymbol{u}_e \end{bmatrix} + \begin{bmatrix} M\boldsymbol{I}_{ion}(\boldsymbol{v},\boldsymbol{w},\boldsymbol{c}) \\ \boldsymbol{0} \end{bmatrix} = \begin{bmatrix} \boldsymbol{0} \\ M\boldsymbol{I}^e_{app} \end{bmatrix}, \\ \dfrac{d\boldsymbol{w}}{dt} = \boldsymbol{R}(\boldsymbol{v},\boldsymbol{w}), \\ \dfrac{d\boldsymbol{c}}{dt} = \boldsymbol{S}(\boldsymbol{v},\boldsymbol{w},\boldsymbol{c}), \end{cases}
$$

with block mass and stiffness matrices

$$
\mathbb{M} = \begin{bmatrix} M & 0 \\ 0 & 0 \end{bmatrix}, \qquad \mathbb{A} = \begin{bmatrix} A_i & A_i \\ A_i & A_i + A_e \end{bmatrix}.
$$

Here $\boldsymbol{v}, \boldsymbol{u}_e, \boldsymbol{w} = (\boldsymbol{w}_1, \ldots, \boldsymbol{w}_{N_w})^T$, $\boldsymbol{c} = (\boldsymbol{c}_1, \ldots, \boldsymbol{c}_{N_c})^T$, $\boldsymbol{R}(\boldsymbol{v},\boldsymbol{w}) = (R_1(\boldsymbol{v},\boldsymbol{w}), \ldots, R_{N_w}(\boldsymbol{v},\boldsymbol{w}))^T$, $\boldsymbol{S}(\boldsymbol{v},\boldsymbol{w},\boldsymbol{c}) = (S_1(\boldsymbol{v},\boldsymbol{w},\boldsymbol{c}), \ldots, S_{N_c}(\boldsymbol{v},\boldsymbol{w},\boldsymbol{c}))^T$, are the coefficient vectors of the finite element approximations of u_i, u_e, v, w_r, c_r, $R_r(v, w_1, \ldots, w_{N_w})$, $S_r(v, w_1, \ldots, w_{N_w}, c_1, \ldots, c_{N_c})$, respectively. In our case of isoparametric trilinear finite elements, these are the vectors of nodal values of these functions.

3.2 – *Time discretization*

The time discretization of the Bidomain equations can be performed using either implicit, semi-implicit or explicit schemes, requiring accordingly vector updates or the solution of a non-linear or linear system. Fully implicit methods in time have been considered e.g. in [19, 17, 18, 28]. The advantage of implicit methods is that they do not require stability constraints on the choice of the time step, but they are very expensive, because at each time step one has to solve a non-linear system. A good compromise between stability and efficiency is obtained using linear implicit methods, studied e. g. in [7, 8, 17], which require at each time step the solution of 2-4 linear systems, or semi-implicit methods, studied e.g. in [5, 9, 29, 38]. For a detailed comparative study on the stability and accuracy of several Bidomain time discretizations (implicit, semi-implicit, explicit), we refer to the recent work [9]. However, the most popular technique is based on operator splitting, i.e. on separating the diffusion operator, associated with conduction in the media, from the reaction operator, associated with the ionic current, gating and ionic concentrations dynamics. The advantage of splitting methods is to allow different numerical schemes for the diffusion and the reaction terms in order to maximize computational efficiency and eliminate complex dependency between variables. The disadvantage is a loss of accuracy, because the simultaneous dependency between variables is neglected.

In this work, we consider an implicit-explicit (IMEX) strategy, based on decoupling the ODEs from the PDEs and on treating the linear diffusion terms

implicitly and the non-linear reaction terms explicitly. The implicit treatment of the diffusion term is needed in order to avoid a stability constraint on the time step Δt induced by the fine mesh size h. Nevertheless, due to the explicit treatment of the reaction terms, stability could be preserved for a time step Δt satisfying a condition of CFL type. To our knowledge, a theoretical and numerical investigation of stability properties of IMEX methods for the Bidomain model coupled to the LR1 membrane model is still lacking in literature. Some rigorous results on stability of IMEX methods for the Bidomain system coupled to the Fitzhugh-Nagumo membrane model are presented in [9].

The equations in (4) arising from the discretization of the PDEs are solved as a coupled system. Given $\boldsymbol{w}^n,\ \boldsymbol{c}^n,\ \boldsymbol{v}^n,\ \boldsymbol{u}_e^n$ at the generic time step n:

– we first solve the ODEs system by computing by Implicit Euler the new gating variables $\boldsymbol{w}^{n+1}$ and by Explicit Euler the new ionic concentrations $\boldsymbol{c}^{n+1}$,

– then we solve the PDEs system computing $\boldsymbol{v}^{n+1}$ and $\boldsymbol{u}_e^{n+1}$.

Summarizing in formulae, given $\boldsymbol{w}^n,\ \boldsymbol{c}^n,\ \boldsymbol{v}^n, \boldsymbol{u}_e^n$, the scheme is

$$\begin{aligned}
\boldsymbol{w}^{n+1} - \Delta t\, \boldsymbol{R}(\boldsymbol{v}^n, \boldsymbol{w}^{n+1}) &= \boldsymbol{w}^n \\
\boldsymbol{c}^{n+1} &= \boldsymbol{c}^n + \Delta t\, \boldsymbol{S}(\boldsymbol{v}^n, \boldsymbol{w}^{n+1}, \boldsymbol{c}^n) \\
(c_t \mathbb{M} + \mathbb{A}) \begin{bmatrix} \boldsymbol{v}^{n+1} \\ \boldsymbol{u}_e^{n+1} \end{bmatrix} &= c_t \mathbb{M} \begin{bmatrix} \boldsymbol{v}^n \\ \boldsymbol{u}_e^n \end{bmatrix} + \begin{bmatrix} -M\boldsymbol{I}_{ion}(\boldsymbol{v}^n, \boldsymbol{w}^{n+1}, \boldsymbol{c}^{n+1}) \\ M\boldsymbol{I}_{app}^{e,n+1} \end{bmatrix},
\end{aligned}$$

where $c_t = \dfrac{c_m}{\Delta t}$. As a consequence, at each time step, we solve one linear system with unknowns $(\boldsymbol{v}^{n+1}, \boldsymbol{u}_e^{n+1})$. Because the iteration matrix is symmetric positive semi-definite, the iterative method employed is the preconditioned conjugate gradient (PCG) method. Due to the ill-conditioning of the iteration matrix and the large number of unknowns required by realistic simulations of cardiac excitation in three-dimensional domains, a scalable and efficient preconditioner is required. We will compare two Block Preconditioners, both based on approximating the diagonal blocks of the linear system matrix

$$\mathcal{A}_{bid} := c_t \mathbb{M} + \mathbb{A} = \begin{bmatrix} c_t \mathrm{M} + \mathrm{A}_i & \mathrm{A}_i \\ \mathrm{A}_i & \mathrm{A} \end{bmatrix}$$

with Block Jacobi or Algebraic Multigrid or Multilevel Hybrid Schwarz preconditioners.

4. – The Multilevel Hybrid Schwarz preconditioner

Let $\mathcal{T}_i$, $i = 0, \ldots, \ell - 1$ be a family of ℓ nested triangulations of Ω, coarsening from $\ell - 1$ to 0, hence $\mathcal{T}_0$ represents the coarsest level of discretization and $\mathcal{T}_{\ell-1}$

the finest one. Let us define the matrix $\mathrm{A} = c_t M + A_i$ or $\mathrm{A} = A_i + A_e$ and the restriction operators $\mathrm{R}^{(i)}$ from level $\mathcal{T}_{i+1}$ to level $\mathcal{T}_i$. With these definitions, set the matrices

$$\mathrm{A}^{(i)} := \mathrm{R}^{(i)} \mathrm{A} \mathrm{R}^{(i)^T},$$

thus $\mathrm{A}^{(\ell-1)} = \mathrm{A}$. We then decompose Ω into N overlapping subdomains, hence each grid $\mathcal{T}_i$ is decomposed into N overlapping subgrids $\Omega_k^{(i)}$ for $k = 1, \ldots, N$, such that the overlap $\delta^{(i)}$ at level $i = 1, \ldots, \ell - 1$ is equal to the mesh size $h^{(i)}$ of the grid $\mathcal{T}_i$. Let $R_k^{(i)}$, for $k = 1, \ldots, N$, be the restriction operators from $\mathcal{T}_i$ to $\Omega_k^{(i)}$, that is $R_k^{(i)}$ returns the vector of all the coefficients associated with domain $\Omega_k^{(i)}$. Define the matrix

$$\mathrm{A}_k^{(i)} := \mathrm{R}_k^{(i)} \mathrm{A}^{(i)} \mathrm{R}_k^{(i)^T},$$

i.e. the subblock matrix of $\mathrm{A}^{(i)}$ associated with domain $\Omega_k^{(i)}$. The action of the ℓ-level hybrid Schwarz preconditioner (MHS(ℓ)) on a given fine level residual $\boldsymbol{r}^{(\ell-1)}$ of the PCG iteration is computed as:

$$\begin{aligned}
&\boldsymbol{u}^{(\ell-1)} \leftarrow \sum_{k=1}^{N} \mathrm{R}_k^{(\ell-1)^T} \mathrm{A}_k^{(\ell-1)^{-1}} \mathrm{R}_k^{(\ell-1)} \boldsymbol{r}^{(\ell-1)} \\
&\boldsymbol{r}^{(\ell-2)} \leftarrow \mathrm{R}^{(\ell-2)} (\boldsymbol{r} - \mathrm{A}^{(\ell-1)} \boldsymbol{u}^{(\ell-1)}) \\
&\boldsymbol{u}^{(\ell-2)} \leftarrow \sum_{k=1}^{N} \mathrm{R}_k^{(\ell-2)^T} \mathrm{A}_k^{(\ell-2)^{-1}} \mathrm{R}_k^{(\ell-2)} \boldsymbol{r}^{(\ell-2)} \\
&\boldsymbol{r}^{(\ell-3)} \leftarrow \mathrm{R}^{(\ell-3)} (\boldsymbol{r}^{(\ell-2)} - \mathrm{A}^{(\ell-2)} \boldsymbol{u}^{(\ell-2)}) \\
&\ldots \\
&\boldsymbol{u}^{(0)} \leftarrow \mathrm{A}^{(0)^{-1}} \boldsymbol{r}^{(0)} \\
&\boldsymbol{u}^{(1)} \leftarrow \boldsymbol{u}^{(1)} + \mathrm{R}^{(0)^T} \boldsymbol{u}^{(0)} \\
&\boldsymbol{u}^{(1)} \leftarrow \boldsymbol{u}^{(1)} + \sum_{k=1}^{N} \mathrm{R}_k^{(1)^T} \mathrm{A}_k^{(1)^{-1}} \mathrm{R}_k^{(1)} (\boldsymbol{r}^{(1)} - \mathrm{A}^{(1)} \boldsymbol{u}^{(1)}) \\
&\ldots \\
&\boldsymbol{u}^{(\ell-1)} \leftarrow \boldsymbol{u}^{(\ell-1)} + \mathrm{R}^{(\ell-2)^T} \boldsymbol{u}^{(\ell-2)} \\
&\boldsymbol{u}^{(\ell-1)} \leftarrow \boldsymbol{u}^{(\ell-1)} + \sum_{k=1}^{N} \mathrm{R}_k^{(\ell-1)^T} \mathrm{A}_k^{(\ell-1)^{-1}} \mathrm{R}_k^{(\ell-1)} (\boldsymbol{r}^{(\ell-1)} - \mathrm{A}^{(\ell-1)} \boldsymbol{u}^{(\ell-1)}) \\
&\boldsymbol{u} \leftarrow \boldsymbol{u}^{(\ell-1)}
\end{aligned}$$

We remark that MHS(ℓ) is additive on each level among the subdomains and multiplicative among the levels.

5. – The Block-Diagonal and Block-Factorized preconditioners

Serial block preconditioners for the Bidomain system have been studied by Pennacchio and Simoncini [23, 24]. Here we extend their study to the parallel context and additionally we combine block preconditioners with multilevel domain decomposition techniques on each block, obtaining convergence rate estimates that depend on both the block parameter γ defined in (7) below and domain decomposition parameters. Denoting by

$$A = \begin{bmatrix} \mathrm{A}_{11} & \mathrm{A}_{12} \\ \mathrm{A}_{12} & \mathrm{A}_{22} \end{bmatrix}$$

the Bidomain matrix $\mathcal{A}_{bid}$, we will consider the following classical block preconditioners for A (see Axelsson [1]):

– the Block-Diagonal preconditioner

$$B_D = \begin{bmatrix} \mathrm{B}_1 & 0 \\ 0 & \mathrm{B}_2 \end{bmatrix}, \tag{5}$$

– the Block-Factorized preconditioner

$$B_F = \begin{bmatrix} \mathrm{I} & 0 \\ \mathrm{A}_{12}\mathrm{B}_1^{-1} & \mathrm{I} \end{bmatrix} \begin{bmatrix} \mathrm{B}_1 & \mathrm{A}_{12} \\ 0 & \mathrm{B}_2 \end{bmatrix}. \tag{6}$$

The main abstract results for these preconditioners are given in the following two propositions, see Axelsson [1] for a proof. For both propositions, we define the constant

$$\gamma^2 = \sup_{\boldsymbol{v} \in \mathbb{R}^n \setminus Ker(\mathrm{A}_{22})} \frac{\boldsymbol{v}^T \mathrm{A}_{12} \mathrm{A}_{11}^{-1} \mathrm{A}_{12} \boldsymbol{v}}{\boldsymbol{v}^T \mathrm{A}_{22} \boldsymbol{v}} \tag{7}$$

and the function $\phi(x) = \dfrac{1}{2}(1+x) + \sqrt{\dfrac{1}{4}(1-x^2) + x\gamma^2}$.

Proposition 5.1 (Axelsson [1, Th. 9.3]). – *If* $\alpha_1 \mathrm{A}_{11} \le \mathrm{B}_1 \le \alpha_2 \mathrm{A}_{11}$, $\beta_1 \mathrm{A}_{22} \le \mathrm{B}_2 \le \beta_2 \mathrm{A}_{22}$, *with* $\alpha_2 \ge \beta_2$, *then*

$$\kappa_2(B_D^{-1} A) \le \frac{\alpha_2}{\alpha_1(1-\gamma^2)} \phi\left(\frac{\alpha_1}{\beta_1}\right) \phi\left(\frac{\beta_2}{\alpha_2}\right).$$

Proposition 5.2 (Axelsson [1, Th. 9.5]). – *If* $\alpha_1 \mathrm{A}_{11} \le \mathrm{B}_1 \le \alpha_2 \mathrm{A}_{11}$, $\delta_1 \mathrm{A}_{22} \le \mathrm{S}_2 \le \delta_2 \mathrm{A}_{22}$, *where* $\mathrm{S} = \mathrm{B}_2 + \mathrm{A}_{12}\mathrm{B}_1^{-1}\mathrm{A}_{12}$, *with* $\alpha_2 \ge 1 \ge \alpha_1 > \gamma^2$, $\delta_2 \ge 1 \ge \delta_1 > \gamma^2$, *then*

$$\lambda_{min}(B_F^{-1} A) \ge \left(1 + \frac{\max\{\alpha_2, \delta_2\} - 1}{1-\gamma^2} \phi(r_2)\right)^{-1},$$

where $r_2 = \min\left\{\dfrac{\alpha_2-1}{\delta_2-1}, \dfrac{\delta_2-1}{\alpha_2-1}\right\}$, *and* $\alpha_2 > 1$ *and/or* $\delta_2 > 1$,

$$\lambda_{max}(B_F^{-1}A) \leq \left(1 - \frac{1-\min\{\alpha_1,\delta_1\}}{1-\gamma^2}\phi(r_1)\right)^{-1},$$

where $r_1 = \min\left\{\dfrac{1-\alpha_1}{1-\delta_1}, \dfrac{1-\delta_1}{1-\alpha_1}\right\}$, *and* $\alpha_1 < 1$ *and/or* $\delta_1 < 1$.

We now define the diagonal blocks $\mathrm{B}_1, \mathrm{B}_2$ of our block preconditioners (5), (6) as Multilevel Hybrid Schwarz (MHS) preconditioners for each scalar component. Therefore we define

$$\begin{aligned} B_1^{-1} &= \text{scalar MHS preconditioner for } c_t\mathrm{M} + \mathrm{A}_i, \\ B_2^{-1} &= \text{scalar MHS preconditioner for } \mathrm{A}_i + \mathrm{A}_e. \end{aligned} \tag{8}$$

In the numerical section, we will compare these MHS block preconditioners with the analogous Block Jacobi (BJ) block preconditioners, where

$$\begin{aligned} B_1^{-1} &= \text{scalar BJ preconditioner for } c_t\mathrm{M} + \mathrm{A}_i, \\ B_2^{-1} &= \text{scalar BJ preconditioner for } \mathrm{A}_i + \mathrm{A}_e, \end{aligned} \tag{9}$$

and with the Algebraic Multigrid (AMG) block preconditioners where

$$\begin{aligned} B_1^{-1} &= \text{scalar AMG preconditioner for } c_t\mathrm{M} + \mathrm{A}_i, \\ B_2^{-1} &= \text{scalar AMG preconditioner for } \mathrm{A}_i + \mathrm{A}_e. \end{aligned} \tag{10}$$

LEMMA 5.1. – *The condition number of the block - diagonal preconditioned operator with MHS scalar blocks* (8) *is bounded by*

$$\kappa_2(B_D^{-1}A) \leq c \max_{1\leq k\leq L-1}\left(1 + \frac{h^{(k-1)}}{\delta^{(k)}}\right)\frac{1+\gamma}{1-\gamma},$$

where $h^{(k-1)}$ *is the mesh size of the* $(k-1)$*-level grid and* $\delta^{(k)}$ *is the overlap size of the k-level grid.*

Lemma 5.1 shows that, in addition to the standard domain decomposition parameters $h^{(k-1)}$ and $\delta^{(k)}$, the convergence of the Block-Diagonal preconditioner B_D depends on the parameter γ, which in turn depends only on the original Bidomain blocks. Pennacchio and Simoncini [23] have shown that

$$\gamma^2 \leq (1 + \lambda_{min}(\mathrm{A}_e, \mathrm{A}_i))^{-1},$$

where $\lambda_{min}(\mathrm{A}_e, \mathrm{A}_i)$ is the minimum eigenvalue of $\mathrm{A}_e\mathrm{A}_i^{-1}$ (see [23, Lemma 4.1]) and numerical experiments seem to indicate that γ is close to $1/2$, so the bound of Lemma 5.1 is satisfactory.

LEMMA 5.2. – *The extreme eigenvalues of the Block-Factorized preconditioned operator with MHS scalar blocks* (8) *are bounded by*

$$\lambda_{min}(B_F^{-1}A) \geq \left(1 + 2\frac{c \max\limits_{1\leq k\leq L-1}\left(1+\dfrac{h^{(k-1)}}{\delta^{(k)}}\right) + N_c}{1-\gamma^2} \right)^{-1},$$

$$\lambda_{max}(B_F^{-1}A) \leq \left(1 - \frac{1-(N_c+1)^{-1}}{1-\gamma} \right)^{-1},$$

where N_c is the number of colors of the subdomains partition.

These bounds are pessimistic because, due to Prop. 5.2, they require that $\gamma^2 < \delta_1$ and predict a large condition number when γ^2 approaches δ_1, while our numerical results seem to indicate that the same considerations on γ for the Block-Diagonal case also hold for the Block-Factorized case.

6. – Numerical results

In this section, we present the results of parallel numerical experiments performed on the Linux Cluster HP of the Department of Mathematics of the University of Milan. Our FORTRAN code is based on the parallel library PETSc [2], from the Argonne National Laboratory.

The Bidomain system coupled to the LR1 model is integrated by the coupled and uncoupled Implicit-Explicit methods described in the previous sections. The values of the coefficients and parameters in the LR1 model are given in the original paper [16]. The linear systems at each time step are solved by the preconditioned conjugate gradient (PCG) method, using as stopping criterion a 10^{-6} reduction of the relative residual l^2-norm. The preconditioners used are the Block-Diagonal and Block-Factorized preconditioners with Block Jacobi (BJ), Algebraic Multigrid (AMG) and 4-level Hybrid Schwarz (MHS(4)) approximations of the diagonal blocks of the original Bidomain system matrix. The AMG solver is based on the BoomerAMG algorithm [12], provided in the Hypre library [13].

Domain geometry and fiber structure.

The domain Ω is the image of a cartesian slab using ellipsoidal coordinates, yielding a portion of truncated ellipsoid. The family of truncated ellipsoids is

described by the parametric equations

$$\begin{cases} x = a(r)\cos\theta\cos\phi & \phi_{min} \le \phi \le \phi_{max}, \\ y = b(r)\cos\theta\sin\phi & \theta_{min} \le \theta \le \theta_{max}, \\ z = c(r)\sin\theta & 0 \le r \le 1, \end{cases}$$

where $a(r) = a_1 + r(a_2 - a_1)$, $b(r) = b_1 + r(b_2 - b_1)$, $c(r) = c_1 + r(c_2 - c_1)$, and $a_1 = 1.5$, $a_2 = 2.7$, $b_1 = 1.5$, $b_2 = 2.7$, $c_1 = 4.4$, $c_2 = 5$ are given coefficients (all in cm) determining the main axes of the ellipsoid. The fibers rotate intramurally linearly with the depth for a total amount of 90° proceeding counterclockwise from epicardium to endocardium. More precisely, in a local ellipsoidal reference system ($\boldsymbol{e}_\phi$, $\boldsymbol{e}_\theta$, $\boldsymbol{e}_r$), the fiber direction $\boldsymbol{a}_l(\boldsymbol{x})$ at a point $\boldsymbol{x}$ is given by

$$\boldsymbol{a}_l(\boldsymbol{x}) = \boldsymbol{e}_\phi \cos\alpha(r) + \boldsymbol{e}_\theta \sin\alpha(r), \quad \text{with} \quad \alpha(r) = \frac{2}{3}\pi(1-r) - \frac{\pi}{4}, \qquad 0 \le r \le 1.$$

Conductivity coefficients.

The values of the conductivity coefficients in (2) used in all the numerical tests are the following:

$$\begin{aligned} &\sigma_l^i = 3 \cdot 10^{-3} \Omega^{-1} cm^{-1} && \sigma_l^e = 2 \cdot 10^{-3} \Omega^{-1} cm^{-1} \\ &\sigma_t^i = 3.1525 \cdot 10^{-4} \Omega^{-1} cm^{-1} && \sigma_t^e = 1.3514 \cdot 10^{-3} \Omega^{-1} cm^{-1} \\ &\sigma_n^i = 3.1525 \cdot 10^{-5} \Omega^{-1} cm^{-1} && \sigma_n^e = 6.757 \cdot 10^{-4} \Omega^{-1} cm^{-1}. \end{aligned}$$

Mesh hierarchy.

In the case of the MHS preconditioner, the coarse meshes are constructed by progressively halving the number of elements in each coordinate direction.

Stimulation site, initial and boundary conditions.

The depolarization process is started by applying a stimulus of $I_{app}^e = -200\ mA/cm^3$ lasting $1\ ms$ on the face of the domain modeling the endocardial surface. The initial conditions are at resting values for all the potentials and LR1 gating variables, while the boundary conditions are for insulated tissue. In all simulations, the fine mesh size is $h = 0.01\ cm$. The time step size is $\Delta t = 0.05\ ms$.

6.1 – *Test 1: weak scaling on ellipsoidal subdomains*

We compare the performance of MHS(4), BJ and AMG Block-Diagonal and Block-Factorized preconditioners on a weak scaling test with increasing ellipsoidal domains. The local size of each subdomain on the finest mesh is kept fixed at the value 48^3 and each subdomain is assigned to one processor. The number of subdomains (hence number of processors) is increased from 2 to 32 forming increasing domains that are portions of a truncated ellipsoidal domain. With these data, the global size of the discrete Bidomain system increases from 465794 dof with 8 processors to 7226306 dof with 32 processors.

The results reported in Table 1 show that both the AMG and MHS block preconditioners are scalable, with the condition number and PCG iterations which remain bounded when increasing the number of processors. Instead, the BJ block preconditioners are not scalable, because the condition number and iteration counts grow with the number of subdomains. In terms of computational performance, the MHS block preconditioners are clearly the most efficient, with CPU time reductions of about 30% and 50% with respect to the BJ and AMG solvers, respectively.

TABLE 1. – Test 1, weak scaling on ellipsoidal domains for Block-Diagonal and Block-Factorized preconditioners with Block Jacobi (BJ), Algebraic Multigrid (AMG) and 4-level Hybrid Schwarz (MHS(4)) approximations of the diagonal blocks of the original Bidomain system matrix. Average condition numbers (κ_2), PCG iteration counts (it.) and CPU times in seconds per time step for each preconditioner as a function of the number of processors/subdomains (procs).

Weak scaling test, Block-Diagonal

		BJ			AMG			MHS(4)		
procs	dof	κ_2	it	time	κ_2	it	time	κ_2	it	time
2	465794	4.05e+3	132	12.41	6.76	13	8.13	2.21	7	3.69
4	922082	5.99e+3	165	33.54	15.39	20	22.76	24.14	26	22.74
8	1825346	5.58e+3	211	75.63	13.92	21	51.09	20.73	25	38.25
16	3631874	5.66e+3	205	74.15	13.89	21	54.28	20.21	23	35.15
32	7226306	1.04e+4	268	97.52	12.22	21	58.58	17.17	22	34.82

Weak scaling test, Block-Factorized

		BJ			AMG			MHS(4)		
procs	dof	κ_2	it	time	κ_2	it	time	κ_2	it	time
2	465794	3.91e+3	127	18.81	4.13	9	6.46	1.83	5	2.83
4	922082	5.16e+3	152	39.44	13.83	18	21.75	24.01	23	19.51
8	1825346	4.79e+3	193	101.42	11.21	19	48.62	19.07	23	39.42
16	3631874	4.81e+3	185	98.08	11.23	19	51.83	16.02	20	35.04
32	7226306	8.79e+3	244	129.41	9.90	18	54.73	13.64	19	33.92

6.2 – *Test 2: comparison of the BJ, AMG and MHS(4) block preconditioners on a complete cardiac cycle simulation*

We now compare the block preconditioners on a complete heartbeat (400 *ms*) in a portion of ellipsoid, modeling half of the left ventricle, discretized by a Q_1 structured finite element grid of $128 \times 64 \times 64$ elements (1090050 *dof*). The simulations are run on 16 processors. The time step size is changed according to the adaptive strategy described in [5].

TABLE 2. – Test 2, comparison on a whole heart beat simulation of Block-Diagonal and Block-Factorized preconditioners with Block Jacobi (BJ), Algebraic Multigrid (AMG) and 4-level Hybrid Schwarz (MHS(4)) approximations of the diagonal blocks of the original Bidomain system matrix. Average condition numbers (κ_2), PCG iteration counts (it.) and CPU times in seconds per time step and total CPU times in hours and minutes.

Whole heart beat test								
	Block-Diagonal				Block-Factorized			
	κ_2	it	time	Ttime	κ_2	it	time	Ttime
BJ	2.61e+3	161	16.51 s	5 h 36 m	1.99e+3	138	20.91 s	7 h 6 m
AMG	38.08	26	16.94 s	5 h 45 m	26.59	22	15.64 s	5 h 18 m
MHS(4)	50.43	31	13.00 s	4 h 19 m	42.68	27	13.25 s	4 h 25 m

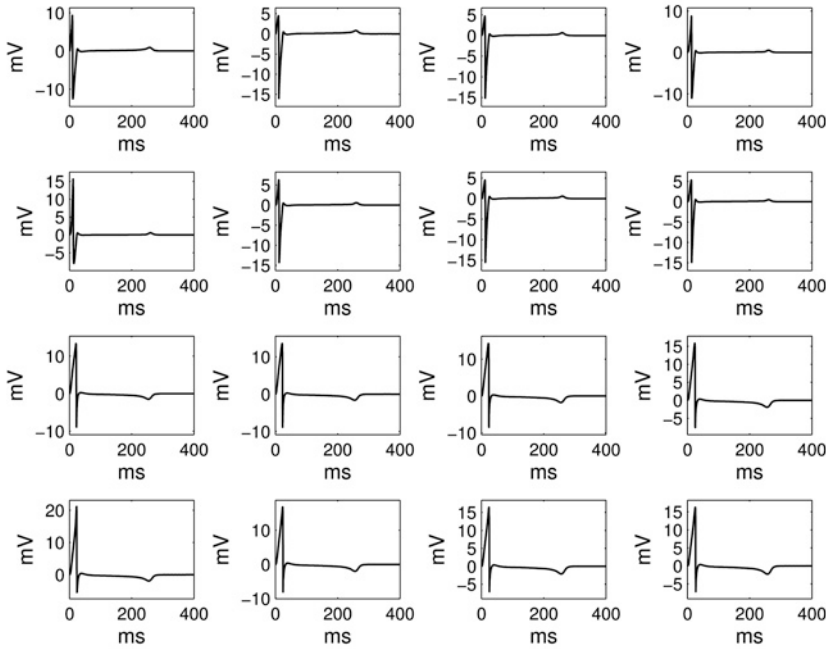

Fig. 1 – Test 2, time (ms) evolutions of the extracellular potential u_e (mV) in 16 epicardial sites.

The results in Table 2 confirm that the MHS block preconditioners are the most efficient, with CPU time reductions of about 20% with respect to the BJ and AMG solvers. Moreover, the BJ and AMG Block-Diagonal preconditioners are comparable, while the BJ Block-Factorized preconditioner is clearly slower than the AMG Block-Factorized preconditioner. Fig. 1 reports the time evolution of the extracellular potential u_e (the electrocardiograms) in 16 epicardial sites.

7. – Conclusion

We have studied the scalability and efficiency of Multilevel Hybrid Schwarz (MHS) Block-Diagonal and Block-Factorized preconditioners for the Bidomain model of the cardiac bioelectric activity. The three-dimensional parallel numerical tests performed on a Linux cluster have shown that the MHS block preconditioners are scalable and about 20-50% (depending on the simulation) more efficient than Block Jacobi and Algebraic Multigrid block preconditioners.

Acknowledgments. The author thanks Piero Colli Franzone and Luca Pavarino for introducing him to the field of Mathematical Cardiac Electrophysiology and for many helpful discussions and suggestions.

REFERENCES

[1] O. Axelsson, *Iterative Solution Methods*, Cambridge University Press, 1994.

[2] S. Balay - K. Buschelman - W. D. Gropp - D. Kaushik - M. Knepley - L. Curfman McInnes - B. F. Smith - H. Zhang, *PETSc Users Manual.Tech. Rep. ANL-95/11 - Revision 2.1.5*, Argonne National Laboratory, 2002.

[3] M. Boulakia - S. Cazeau - M. A. Fernandez - J.-F. Gerbeau - N. Zemzemi, *Mathematical modeling of electrocardiograms: a numerical study*. Ann. Biomed. Eng., **38** (3) (2010), 1071-1097.

[4] R. H. Clayton - O. Bernus - E. M. Cherry - H. Dierckx - F. H. Fenton - L. Mirabella - A. V. Panfilov - F. B. Sachse - G. Seemann - H. Zhang, *Models of cardiac tissue electrophysiology: Progress, challenges and open questions*. Progr. Biophys. Molec. Biol., **104** (2011), 22-48.

[5] P. Colli Franzone - L. F. Pavarino, *A parallel solver for reaction-diffusion systems in computational electrocardiology*. Math. Mod. Meth. Appl. Sci., **14** (6) (2004), 883-911.

[6] P. Colli Franzone - L. F. Pavarino - B. Taccardi, *Simulating patterns of excitation, repolarization and action potential duration with cardiac bidomain and monodomain models*. Math. Biosci., **197** (1) (2005), 33-66.

[7] P. Colli Franzone - P. Deuflhard - B. Erdmann - J. Lang - L. F. Pavarino, *Adaptivity in space and time for reaction-diffusion systems in Electrocardiology*. SIAM J. Sci. Comput., **28** (3) (2006), 942-962.

[8] P. Deuflhard - B. Erdmann - R. Roitzsch - G. T. Lines, *Adaptive finite element simulation of ventricular fibrillation dynamics*. Comput. Visual. Sci., **12** (5) (2009), 201-205.

[9] M. Ethier - Y. Bourgault, *Semi-implicit time-discretization schemes for the Bidomain model*. SIAM J. Numer. Anal., **46** (5) (2008), 2443-2468.

[10] L. Gerardo Giorda - L. Mirabella - F. Nobile - M. Perego - A. Veneziani, *A model-based block-triangular preconditioner for the Bidomain system in electrocardiology*. J. Comp. Phys., **228** (10) (2009), 3625-3639.

[11] L. Gerardo Giorda - M. Perego - A. Veneziani, *Optimized Schwarz coupling of Bidomain and Monodomain models in electrocardiology*, Math. Model. Numer. Anal., **45** (2011), 309-334.

[12] V. Henson - U. Yang, *BoomerAMG: a parallel algebraic multigrid solver and preconditioner*. Appl. Numerical Math., **41** (2002), 155-177.

[13] *HypreHigh Performance Preconditioners Users Manual Center for Applied Scientific Computing*, Lawrence Livermore National Laboratory, Tech. Rep. Software Version: 1.6.0, Jul. 27, 2001.

[14] I. J. LeGrice - B. H. Smaill - L. Z. Chai - S. G. Edgar - J. B. Gavin - P. J. Hunter, *Laminar structure of the heart: ventricular myocyte arrangement and connective tissue architecture in the dog*. Am. J. Physiol. Heart Circ. Physiol., **269** (38) (1995), H571-H582.

[15] S. Linge - J. Sundnes - M. Hanslien - G. T. Lines - A. Tveito, *Numerical solution of the bidomain equations*. Phil. Trans. R. Soc. A, **367** (1895) (2009), 1931-1950.

[16] C. Luo - Y. Rudy, *A model of the ventricular cardiac action potential: depolarization, repolarization, and their interaction*. Circ. Res., **68** (6) (1991), 1501-1526.

[17] M. Munteanu - L. F. Pavarino, *Decoupled Schwarz algorithms for implicit discretization of nonlinear Monodomain and Bidomain systems*. Math. Mod. Meth. Appl. Sci., **19** (7) (2009), 1065-1097.

[18] M. Munteanu - L. F. Pavarino - S. Scacchi, *A scalable Newton-Krylov-Schwarz method for the Bidomain reaction-diffusion system*. SIAM J. Sci. Comput., **31** (5) (2009), 3861-3883.

[19] M. Murillo - X.-C. Cai, *A fully implicit parallel algorithm for simulating the nonlinear electrical activity of the heart*. Numer. Linear Algebra Appl., **11** (2-3) (2004), 261-277.

[20] L. F. Pavarino - S. Scacchi, *Multilevel additive Schwarz preconditioners for the Bidomain reaction-diffusion system*. SIAM J. Sci. Comput., **31** (1) (2008), 420-443.

[21] L. F. Pavarino - S. Scacchi, *Parallel Multilevel Schwarz and Block Preconditioners for the Bidomain Parabolic-Parabolic and Parabolic-Elliptic Formulations*, SIAM J. Sci. Comput., **33** (4) (2011),1897-1919.

[22] M. Pennacchio - G. Savaré - P. Colli Franzone, *Multiscale modeling for the bioelectric activity of the heart*. SIAM J. Math. Anal., **37** (4) (2006), 1333-1370.

[23] M. Pennacchio - V. Simoncini, *Algebraic multigrid preconditioners for the bidomain reaction-diffusion system*, Appl. Numer. Math., **59** (2009), 3033-3050.

[24] M. Pennacchio - V. Simoncini, *Fast structured AMG preconditioning for the bidomain model in electrocardiology*. SIAM J. Sci. Comput., **33** (2) (2011), 721-745.

[25] G. Plank - M. Liebmann - R. Weber dos Santos - E. J. Vigmond - G. Haase, *Algebraic Multigrid Preconditioner for the Cardiac Bidomain Model*. IEEE Trans. Biomed. Engrg., **54** (4) (2007), 585-596.

[26] M. Potse - B. Dubè - J. Richer - A. Vinet - R. Gulrajani, *A comparison of Monodomain and Bidomain reaction-diffusion models for action potential propagation in the human heart*. IEEE Trans. Biomed. Eng., **53** (12) (2006), 2425-2434.

[27] S. Scacchi, *A hybrid multilevel Schwarz method for the bidomain model*. Comp. Meth. Appl. Mech. Engrg., **197** (45-48) (2008), 4051-4061.
[28] S. Scacchi, *A multilevel hybrid Newton-Krylov-Schwarz method for the Bidomain model of electrocardiology*. Comp. Meth. Appl. Mech. Engrg., **200** (5-8) (2011), 717-725.
[29] K. B. Skouibine - N. Trayanova - P. Moore, *A numerically efficient model for the simulation of defibrillation in an active bidomain sheet of myocardium*. Math. Biosci., **166** (1) (2000), 85-100.
[30] B. F. Smith - P. Bjørstad - W. D. Gropp, *Domain Decomposition: Parallel Multilevel Methods for Elliptic Partial Differential Equations*, Cambridge University Press, 1996.
[31] J. Sundnes - G. T. Lines - K. A. Mardal - A. Tveito, *Multigrid block preconditioning for a coupled system of partial differential equations modeling the electrical activity in the heart*. Comput. Meth. Biomech. Biomed. Engrg., **5** (6) (2002), 397-409.
[32] J. Sundnes - G. T. Lines - A. Tveito, *An operator splitting method for solving the bidomain equations coupled to a volume conductor model for the torso*. Math. Biosci., **194** (2) (2005), 233-248.
[33] A. Toselli - O. B. Widlund, *Domain Decomposition Methods: Algorithms and Theory*. Computational Mathematics, Vol. 34. Springer-Verlag, Berlin, 2004.
[34] M. Veneroni, *Reaction-diffusion systems for the microscopic cellular model of the cardiac electric field*. Math. Meth. Appl. Sci., **29** (2006), 1631-1661.
[35] M. Veneroni, *Reaction-Diffusion systems for the macroscopic Bidomain model of the cardiac electric field*. Nonlin. Anal.-Real World Appl., **10** (2) (2009), 849-868.
[36] E. J. Vigmond - F. Aguel - N. A. Trayanova, *Computational techniques for solving the bidomain equations in three dimensions*. IEEE Trans. Biomed. Engrg., **49** (2002), 1260-1269.
[37] E. J. Vigmond - R. Weber dos Santos - A. J. Prassl - M. Deo - G. Plank, *Solvers for the cardiac bidomain equations*. Progr. Biophys. Molec. Biol., **96** (2008), 3-18.
[38] J. P. Whiteley, *An efficient numerical technique for the solution of the monodomain and bidomain equations*. IEEE Trans. Biomed. Engrg., **53** (11) (2006), 2139-2147.
[39] S. Zampini, *Balancing Neumann-Neumann methods for the cardiac Bidomain model*. Numer. Math., **123** (2) (2013), 363-393.
[40] S. Zampini, *Dual-primal methods for the cardiac bidomain model*. Math. Mod. Meth. Appl. Sci., in press.

Dipartimento di Matematica, Università degli Studi di Milano
Via Saldini 50, 20133 Milano, Italy
E-mail: simone.scacchi@unimi.it

Received November 30, 2012 and in revised form November 2, 2013